

# Thermodielectric effect in dual-frequency cholesteric liquid crystals

Yu-Cheng Hsiao and Wei Lee\*

Institute of Imaging and Biomedical Photonics, College of Photonics, National Chiao Tung University, Guiren Dist., Tainan 71150, Taiwan

## ABSTRACT

Thermodielectric effect in dual-frequency cholesteric liquid crystals (DFCLCs) is an important issue and has rarely been studied in the past. DFCLC materials have many applications such as fast-switching CLCs, light modulators, and tunable photonic devices. However, DFCLCs characteristically need high operation voltage, which hinders their further development in thin-film-transistor operation. Here we present a lower-voltage switching method based on thermodielectric effect. Dielectric heating effect entails applying an electromagnetic wave to occasion dielectric oscillation heating so to induce the increase in crossover frequency. The subsequent change in dielectric anisotropy of the DFCLC permits the switching, with a lower voltage, from the planar state to the focal conic or homeotropic state. Furthermore, we also demonstrate the local deformation of the CLC helical structure achieved by means of the thermodielectric effect. The wavelength of the deformation-induced defect mode can be tuned upon varying the dielectric heating power. The physics and the calculation of dielectric heating in DFCLCs are described.

**Keywords:** cholesteric liquid crystals, dual-frequency liquid crystal, dielectric heating effect, optical stability, photonic devices

## 1. INTRODUCTION

Dual-frequency nematic liquid crystal (DFNLC) was first developed in the 1970s and 1980s.<sup>1</sup> DFCLCs are a LC mixture whose dielectric constant parallel to the molecular axis,  $\epsilon_{\parallel}$ , highly depends on the frequency; and the dielectric constant perpendicular to the molecular axis,  $\epsilon_{\perp}$ , is independent of frequency within the range of tenth of MHz. In other words, dielectric anisotropy of DFNLC is positive in mid-frequency and negative in radio-frequency regions. The specific frequency where dielectric anisotropy cross zero is known as crossover frequency ( $f_c$ ). Based on this feature, DFNLCs have been suggested to extensive applications such as fast-switching optical devices,<sup>2,3</sup> tunable lens,<sup>4</sup> optical retarders,<sup>5</sup> stable system,<sup>6,7</sup> and so forth. In addition, dual-frequency cholesteric liquid crystals (DFCLCs), mixtures that made of DFNLCs and chiral dopants, have a great potential for photonic applications. DFCLCs hold the same frequency-dependent-dielectric-anisotropic characteristic as DFNLCs do which allows DFCLCs can be fast switched among multiple of their peculiar states. Typically, switching CLCs from transparent planar (P) state to opaque focal conic (FC) state relies an AC voltage pulse. The reverse transition, from the FC to P state, however, cannot be directly switched to without an intermediate state. Our previous studies have demonstrated the direct two-way switching between P and FC states with DFCLCs, characterizing a much shorter transition time for practical applications such as light shutters<sup>8,9</sup> and fast-switching color-reflective displays.<sup>10</sup> Nevertheless, DFCLC devices still suffer from two common problems—high operation voltage and thermodielectric effect. In this work, we explore the physics of thermodielectric of a DFCLC system and exploit such effect to switch the states of DFCLCs without necessitating high voltage. Furthermore, through thermodielectric effect a local deformation in the CLC helical structure can be created, serves as a photonic defect layer. The wavelength of the deformation-induced defect modes are tunable by simply applying a frequency-modulated voltage which yields different dielectric heating power.

\*wlee@nctu.edu.tw; phone +886 (0)6 303-2121; fax +886 (0)6 303-2535

## 2. EXPERIMENTAL

The DFNLC material used in this study was MLC-2048 (Merck) with the clearing point at 110 °C and  $\Delta\epsilon = 2.8$  at 1 kHz, 25 °C. The chiral dopant was S-811 (Merck), which was mixed in the DFNLC host at concentrations of 0–15 wt%. The DFCLCs were injected in isotropic phase to the cells by capillary action. Each DFCLC cell was composed of two 1.1-mm-thick indium–tin-oxide glass substrates coated with planar alignment layers, the cell gap was  $11.6 \pm 0.5 \mu\text{m}$ . The rubbed planar alignment layers produce an uniform single-domain texture to the initial P state. To analysis the thermodielectric effect in DFCLCs, the ambient temperature  $T_0$  was fixed at 300 K with a temperature controller. In order to avoid the temperature gradient in the DFCLC cells, we inserted a pair of ~1-mm-thick plastic strips between the cells and the hot plate to stabilize the surrounding air at 300 K. The temperature of the cell surface,  $T_s$ , was measured with a digital thermometer whose thermocouple was attached to the outer surface of the DFCLC cells. The frequency-dependent complex dielectric function  $\epsilon' - i\epsilon''$  was acquired with a computer controlled precision LCR meter (Agilent E4980A), using a 0.5 V<sub>rms</sub> sinusoidal probe voltage, which was lower than the Fréedericksz threshold voltage. The transmission spectra of the DFCLC cells were acquired with a spectrophotometer (Ocean Optics HR2000 +). All experimental data were measured at an ambient temperature of  $299 \pm 1$  K. When a frequency-modulated electric field E is applied across a DFCLC cells, it imposes a torque on the LC director, depending on  $\Delta\epsilon = \epsilon_{\parallel} - \epsilon_{\perp}$ , where  $\epsilon_{\parallel}$  and  $\epsilon_{\perp}$  denote the relative permittivity components in the cases of the director parallel to the electric field and perpendicular to the electric field, respectively. When a low-frequency ( $< f_c$ ) field is applied,  $\Delta\epsilon > 0$  and the director tends to be parallel to the electric field direction. In contrast,  $\Delta\epsilon$  becomes negative and the LC director tends to be perpendicular to the electric field when the DFCLC is in a high-frequency ( $> f_c$ ) field. The strength of the thermodielectric effect is determined by the efficiency of absorption of electromagnetic wave. The dielectric heating effect is manifested through reorientation of the LC molecular dipoles, which is significant at particular frequencies range.<sup>10</sup> The theory and calculation of thermodielectric effect in DFCLCs is discussed.

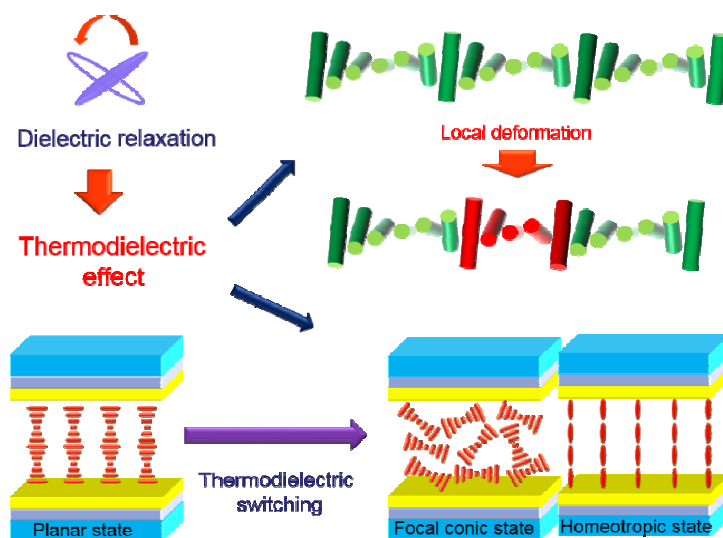


Figure 1. Schematic illustration of the DFCLCs application based on thermodielectric effect.

## 3. RESULTS AND DISCUSSION

### 3.1 The theory of thermodielectric effect in DFCLCs

Figure 2 shows the measured real ( $\epsilon'$ ) and imaginary ( $\epsilon''$ ) parts of the dielectric properties of a DFCLC cell in the frequency range from 1 kHz to 1 MHz. Note that the bias voltages, 0 and 40 V, permitted the measurements of the vertical and parallel dielectric constant components corresponding to  $\epsilon_{\perp}$  and  $\epsilon_{\parallel}$ , respectively. We can observe that  $f_c$  is

about 20 kHz in the conditions of 10 wt% chiral dopant and at 300 K. The frequency spectra can be divided into three main frequency ranges. Firstly, the low frequency regime ( $f < 1$  kHz) demonstrates the induced polarization due to space ion charges; here the ionic behavior is dictated based on the electrode and interface polarizations.<sup>12</sup> Secondly, the frequency range between 1 and 100 kHz is produced with the dielectric orientation behavior of LC molecules.<sup>13</sup> Finally, the dielectric spectra at frequencies about 1 MHz are associated by the pseudo-relaxation originating from the ITO cell configuration.<sup>14</sup> However, the most important is the dielectric orientation behavior of LCs in discussion of thermodielectric effect. The frequency dependence of the complex dielectric constant of a LC, which represents the dielectric storage as well as dielectric loss, follows the Debye-type molecular relaxation

$$\varepsilon^*(\omega) = \varepsilon'(\omega) + i\varepsilon''(\omega),$$

and

$$\varepsilon'(\omega) = \frac{\varepsilon_s - \varepsilon_\infty}{(1 + \omega^2 \tau_D^2)} + \varepsilon_\infty,$$

$$\varepsilon''(\omega) = \frac{(\varepsilon_s - \varepsilon_\infty)\omega\tau_D}{(1 + \omega^2 \tau_D^2)},$$

where  $\varepsilon'(\omega)$  and  $\varepsilon''(\omega)$  are the real and the imaginary parts of the Debye's model.  $\varepsilon_s$  and  $\varepsilon_\infty$  are the low-(static) and the high-frequency dielectric constants of the respective dispersion region. The Debye relaxation time  $\tau_D = 1/\omega_D = 1/2\pi f_D$  can be determined from measurements. The dielectric dissipation, which generates heat in the LC layer, follows from  $\varepsilon''(\omega)$ . The orientation polarization of LCs, associated with the reorientation of permanent electric dipoles, is relatively slow with the time scales ranging from  $10^{-9}$  to  $10^{-2}$  s. The reorientation of dipoles covers the LC reorientation characteristic times about  $10^{-4}$ – $10^{-2}$  s.<sup>13</sup> On the other hand, electronic and molecular polarizations are important to be considered in a much shorter time scale compared with LC reorientation; therefore, we focus on the discussion of the dielectric behavior of LC related to the orientational polarization. Consider such a LC molecule with the longitudinal  $p_l$  and transversal  $p_t$  permanent dipole moments. There are four relaxation modes: mode a is rotations of  $p_t$  around the long axis, and mode b is reorientation of  $p_l$  contributed to the parallel component of dielectric polarization. The mode a has a smaller relaxation time because of the smaller moments of inertia involved. Mode c is associated with conical rotations of  $p_l$  around the director (as the axis of the cone); when the applied electric field is perpendicular to the direction of LC and contributes to the perpendicular component of the dielectric polarization. Finally, mode d is a different mode related with the flip-flops of  $p_l$ . The relaxation time for the mode d is thus significantly larger than the relaxation time of any other mode. Typically, the dielectric heating induced LC flow is in the Mode d. For a describe of DFCLCs, the temperature dependence of  $f_c$  satisfies the Arrhenius equation

$$f_c = A_0 \exp\left(-\frac{E_a}{k_B T}\right),$$

where  $E_a$  is the activation energy of the dielectric relaxation corresponding to the rotation along the molecular short axis,  $A_0$  represents a material constant,  $k_B$  stands for Boltzmann constant, and  $T$  is the absolute temperature. Next, the heat flow rate  $Q_{out}$  at the interface of glass and air as well as cell surface and the surrounding air follows the equation

$$Q_{out} = hA (T_s - T_0),$$

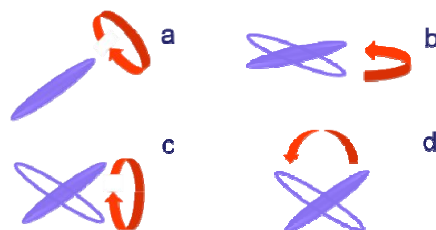


Figure 2. Schematic illustration of orientational relaxation modes for a molecule in DFCLC medium.

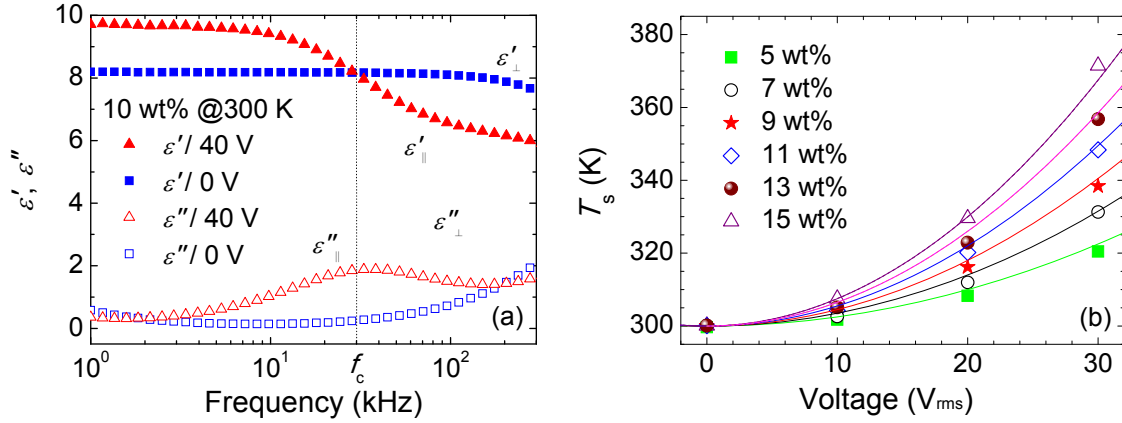


Figure 3. (a) Dielectric dispersion of a DFCLC sample consisting of 10 wt% of chiral dopant at 300 K as well as (b) dielectric heating temperature of DFCLC cells under different applied voltages.

where  $h$  is the heat transfer coefficient and is of  $\sim 40 \text{ W m}^{-2}\text{K}^{-1}$  for the glass substrate<sup>15</sup> and  $A$  is the heat-transfer area and of  $1 \text{ cm}^2$  in this study. If we ignore the small temperature gradient in the DFCLC bulk, the average temperature  $T$  of the DFCLC molecule in thermal equilibrium can be written as<sup>16</sup>

$$T - T_0 = (1 + \text{Bi}) (T_s - T_0),$$

where Biot number of the glass plate is about 0.04 and is the dimensionless, which is negligible to readily deduce  $T = T_s$ . In this study, we used electric field, whose strength  $E = V_{\text{rms}}/d$ , for simplicity, that the electric field is homogeneous in the cell. The dielectric heating power density  $P$  of the LC bulk is thus given by

$$P = \omega \cdot \epsilon_0 \epsilon''(\omega) \cdot E^2 = \frac{2\pi f \epsilon_0 \epsilon''(\omega) V_{\text{rms}}^2}{d^2},$$

where  $\omega$  represents the angular frequency and  $\epsilon_0$  is the permittivity of free space. In this report, the pretilt angle ( $< 2^\circ$ ) is small enough, so the imaginary part of the complex dielectric permittivity is roughly equal to  $\epsilon_0 \epsilon''_{\perp}$  in the initial state. However,  $\epsilon''_{\perp}$  is a linear function of the chiral dopant concentration at 100 kHz based on the past report<sup>11</sup>

$$\epsilon''_{\perp}(c) = \alpha + \beta c,$$

where  $\alpha = 0.016$  and  $\beta = 0.169 \text{ wt}\%^{-1}$  by fitting. In our experiment,  $\epsilon''_{\perp}$  did not explicitly vary with  $T$ . Also note that  $c$  is lower than 16 wt%, beyond which the DFCLC cell became difficult to operate. Now that the LC layer is thin as compared with the glass plates, one can neglect the heat stored in the LC layer itself. As a result, the heat generation  $Q_{\text{in}}$  and dissipation  $Q_{\text{out}}$  can be expressed as  $Q_{\text{in}} = P d A = Q_{\text{out}}$ . The equilibrium temperature of the LC to proceed to

$$T = T_0 + \frac{2\pi f (1 + \text{Bi}) A (\alpha + \beta c) V_{\text{rms}}^2}{hd} \approx T_0 + \gamma f c V_{\text{rms}}^2,$$

where both Bi and  $\alpha$ , in comparison with 1 and  $\beta c$ , respectively, are ignored in the approximation. The relation  $\Delta T = T_s - T_0 \propto f c V_{\text{rms}}^2$  is clearly confirmed by the experimental data as shown in Fig. 3. One can see that the dielectric heating effect is more drastic in the samples with higher CP concentrations as manifested by the higher temperatures measured. It is also clear from Fig. 3 that the experimental data are in good agreement with the simulated results predicted.

### 3.2 Lower operation voltage in DFCLCs based on the thermodielectric effect

DFCLC devices are powerful and have potential to many applications as previous mentioned. However, all DFCLC devices suffer from one common problem—high operation voltage. We employ this thermodielectric effect to switch the cell from the P to the FC or H state by a lower operation voltage. Figure 4 illustrates the electro-optical properties of a DFCLC device (with 10 wt% chiral dopant) between crossed polarizers at low frequency 1 kHz and high frequency 100 kHz. When the low-frequency (1 kHz) voltage is applied, the DFCLC bulk shows positive  $\Delta\varepsilon$ , and the device is initially at the P state. However, through a range of increasing operation voltages, the DFCLC cell exhibits the three main optical states. The colorful brightest one is the initial P state and the scattering FC state appears subsequently at  $\sim 13\text{--}30\text{ V}_{\text{rms}}$ . Finally, the optical texture appears to be the H state when the applied voltage is over  $\sim 30\text{ V}_{\text{rms}}$  as demonstrated in Fig. 4(a). In the voltage ramp-down route, the optical texture changes from the H to FC state and, the device retains the FC state because of bistability. However, when the driving voltage operates at the high frequency (100 kHz), the DFCLC exhibits negative  $\Delta\varepsilon$ . The high-frequency voltage causes severe dielectric heating effect and, in turn, the blue shift of crossover frequency  $f_c$ , eventually inducing the positive dielectric torque. Consequently, the optical texture of the DFCLCs transform from the P state to the FC or H state even when the applied voltage is as low as  $\sim 15\text{ V}_{\text{rms}}$  (Fig. 4(b)). Based on this thermodielectric effect, the operation voltages required for switching the P state is lower compared with that in the convectonal drive scheme. Figure 5 shows the images of real DFCLC cells of thermodielectric induce the molecular flowing under the cross polarizers. We can observe that the P state change to the H state slowly based on the thermodielectric effect. The thermo-induced crossover frequency shifting usually takes time and the optimized condition must be considered. The thermo-induced respond times, defined as the time interval between 10% and 90% of the

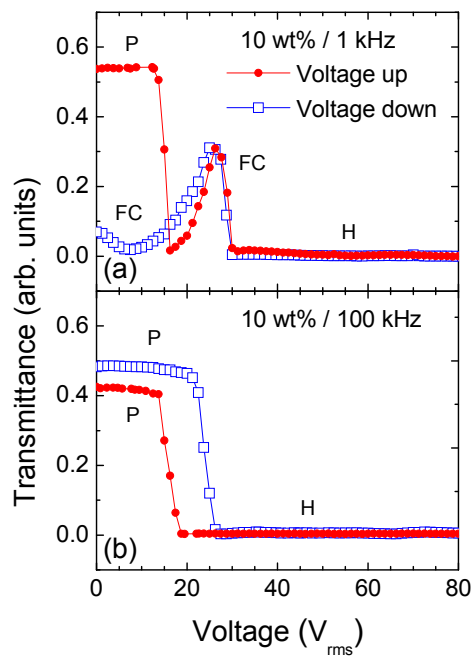


Figure 4. Voltage-dependent transmittance at operation frequencies of (a) 1 kHz and (b) 100 kHz. under crossed polarizers.

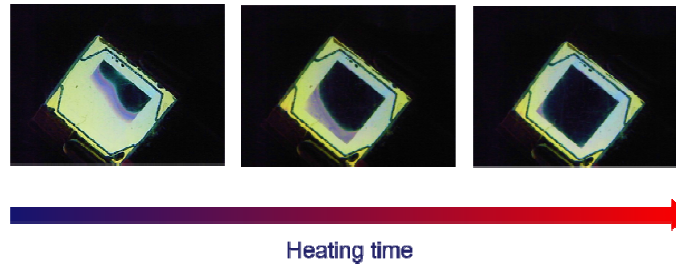


Figure 5. Images of DFCLC cells of dielectric heating effect induced the molecular flowing under the cross polarizers.

Table 1. Transition times from the planar to the homeotropic state with various chiral-dopant concentrations at 15 V<sub>rms</sub> at three different frequencies. (Adopted from Ref. 11.)

Frequency (kHz)	Transition time (ms)				
	8 wt%	9 wt%	10 wt%	11 wt%	12 wt%
50	8 300	5 780	1 420	8 560	–
100	307	283	250	286	344
150	7 350	5 640	1 350	7 530	9 210

minimum–maximum transmittance difference, are showed in Table 1. The transition time increases for an applied lower frequency (say, 50 kHz) due to the weaker dielectric heating effect, and a higher applied frequency (150 kHz) rise the increased transition time because of the long time to shift  $f_c$  to go beyond the higher frequency.

### 3.3 Thermodielectric generation of defect modes in a DFCLC as a “new” photonic device

Photonic crystals (PCs) have been extensively studied in the past.<sup>17,18</sup> In a PC structure, the propagation of light is inhibited under the Bragg condition, generating the so-called photonic band gap (PBG). When an artificial defect layer interrupts the periodicity of the PC structure, photon will confine in the defect layer.<sup>19,20</sup> By inserting a third dielectric material as a defect layer in the PC structure, the defect modes can be generated in the PBG. Utilizing the properties of defect modes, many applications such as optical filters,<sup>20</sup> low-threshold lasers,<sup>21</sup> and fluorescence enhancement devices<sup>21</sup> have been demonstrated. Conventionally, the way to produce defect modes is through prefabrication of a defect layer in a PC; for example, infiltration with liquid crystals (LCs) in a multilayer PC.<sup>3</sup> Such defect modes are often persistent due to the permanent existence of the defect layer. However, CLCs or DFCLCs are one kind of PCs. Thermodielectric effect also can be used as power to generation of defect modes in a DFCLCs. Because of the dielectric heating effect is induced in central DFCLCs layer as gradient distribution.<sup>22</sup>

When polarized light passed through a DFCLC containing a thermodielectro-induced defect layer (TIDL), the same chirality of DFCLCs will induce thermodielectro-induced defect mode (TIDM). It is clear that the left circularly polarized light was reflected within the PBG owing to the left chirality of S811 and the DFCLC to be left-handed. Note that the local deformation-induced change in pitch gave rise to a TIDM window in the PBG for the LCP light. The experimental transmittance spectra of the DFCLC in various heating conditions are also shown in Fig. 6(a). A transmission defect peak originating from the TIDL was observed in the PBG for the LCP case. A pronounced TIDM first appeared at the wavelength of 640 nm as the voltage increased to 40 V<sub>rms</sub>. The spectral peak then blueshifted to 585 nm at 50 V<sub>rms</sub> because of the higher heating power resulting in a shorter pitch length in the middle layer. There is no doubt that the heating time was an important element in the experiment. We measured each spectrum after a voltage was continuously applied for 30 s. In order to further inspect the interaction between the TIDM and the local deformation of the pitch length, simulations results were performed and are depicted in Fig. 6(b). The optical spectral profiles were calculated by using the commercial software DIMOS, which is based on the extended  $2 \times 2$  Jones matrix and  $4 \times 4$  Berreman matrix. However, by decreasing the pitch length from 400 to 290 nm (as labeled in the legend) for a distance of  $1.375 \mu\text{m}$  in the middle, one can see that the simulated data roughly resemble the experimental spectra. A high voltage enhanced the thermodielectric effect. The pitch was, accordingly, shortened and optical path length reduced in the middle (defect) layer at a resulting high temperature, giving a blueshifted TIDM. Figure 7(a) illustrates how the wavelength of the TIDM varied with the energy density and the defect-layer pitch based on previous equation. The

different spatial distributions of the pitch were considered. The DFCLC was divided into 10 layers with the pitch configurations. Since a smoother pitch distribution may be considered as a structure with a thicker defect layer, this can be understood as a result of the increment in effective optical defect thickness. Figure 7(b) depicts an experimental spectrum of a DFCLC under a prolonged heating time ( $50 V_{rms}$  for 50 s) for a smaller temperature gradient in the DFCLC cell. This result is qualitatively in good agreement with the prediction by the simulation results. It is important mentioning that the degree of ideal defect-mode profile is affected by a number of factors. The thermo-hydrodynamics is the main reason to describe the properties of TIDMs. If the dielectric power of heating is higher, the thermo-transition time is faster to switch the states, and then result in the smoother pitch gradient generating the non-ideal plural-peak spectra. On the contrary, under lower applied voltage, the time of ideal one peak mode is longer. It is worth mentioning that TIDMs are difficult to demonstrate or become stabilized. Since the thermoelectric effect induced temperature gradient changed over time before a state of thermal equilibrium was reached, the TIDMs were only observed for a few minutes in DFCLCs. However, this problem can be solved with the polymer stabilization of DFCLCs or CLCs.<sup>6,23</sup>

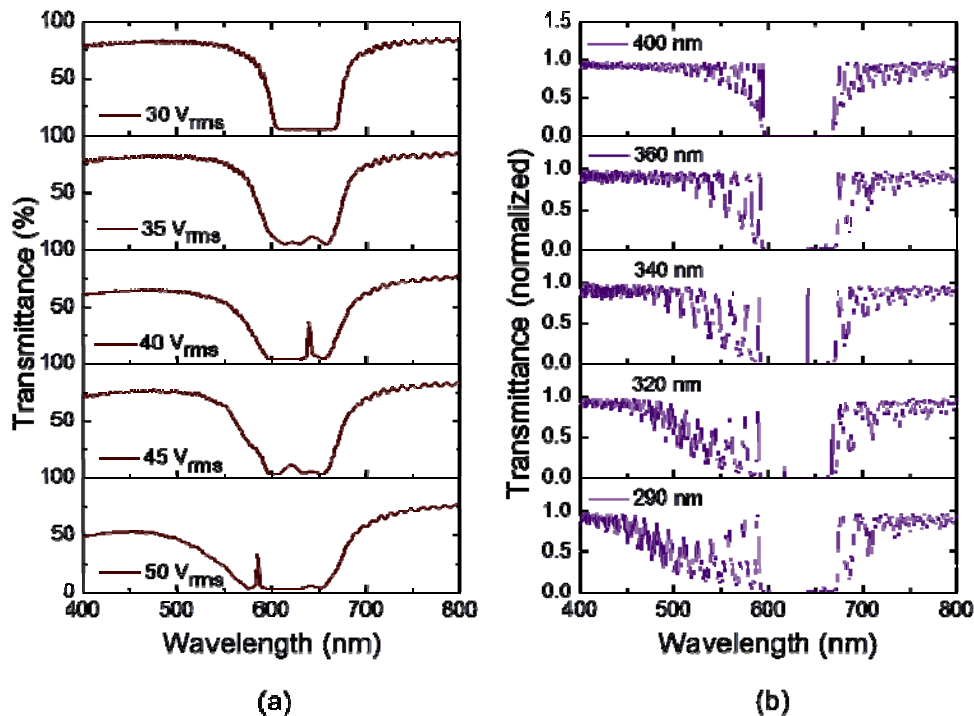


Figure 6. Transmission spectra of DFCLC with thermoelectric induced defect modes (a) at various applied voltages (experimental data) and (b) compared to various pitch values in the middle defect layer in DFCLCs (simulated data). (After Ref. 22.)

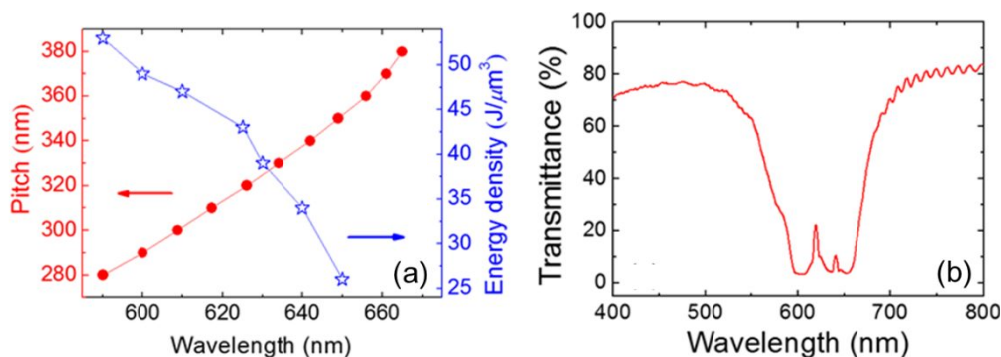


Figure 7. (a) Wavelength of the TIDM varying with the energy density and simulated pitch of the middle defect layer. The symbols show the experimental (blue) and the simulated (red) results. (b) Experimental spectrum obtained in a specific pitch-deformation exhibiting two defect-mode peaks in the PBG. (Adopted from Ref. 22.)

Based on the thermodielectric effect in DFCLCs, we have demonstrated that photonic defect modes can be induced and that the switching and tuning of them can be realized by local deformation of the pitch in the middle layer of a DFCLC cell. An external applied voltage at a high frequency across the DFCLC cell can supply the dielectric heat to induce a defect layer owing to the changed pitch susceptible to the gradient temperature in the DFCLC cell. The TIDMs appeared only when the incident circularly polarized light had the same handedness as the DFCLC. The tuning of the TIDMs can be performed by local compression of the defect-layer helix in DFCLCs, allowing the defect mode to blueshift. Based on controlling the extent of the modulation of the helix condition, a continuous shift of the TIDMs can be realized using the self-organizability of DFCLC without prefabrication of the artificial defect layer. On the basis of thermodielectric effect, various potential applications can be expected such as single-mode lasing, monochromatic selection, on-chip devices and optical communications.

#### 4. CONCLUSION

In summary, the interesting properties of dielectric heating in DFCLCs have been investigated. In a high-frequency-modulated electric field, the thermodielectric effect leads to the increases in temperature resulting in upshift to crossover frequency. Once the sign of dielectric anisotropy is altered the optical states of DFCLCs are changed thereby. Numerous of possible applications were proposed based on this phenomenon, including fast optical modulators, fast shutters and displays. The DFCLCs can be switched from the P state to FC or H state with a low driving voltage at the expense of switching time. Thermodielectric effect can also generate photonic defect modes in a DFCLC. The induced photonic defect mode is tunable in wavelengths and the number of them is controllable. This intriguing effect is believed to have more possibilities than those are proposed in this paper.

#### ACKNOWLEDGMENTS

The authors are grateful for the financial support from the Ministry of Science and Technology, Taiwan under grant Nos. 101-2112-M-009-018-MY3 and 104-2112-M-009-008-MY3.

#### REFERENCES

- [1] Schadt, Martin., "Liquid crystal materials and liquid crystal displays," *Annu. Rev. Mater. Sci.* 27, 305–379 (1997).
- [2] Golovin, A. B., Shiyankovskii, S. V. and Lavrentovich, O. D., "Fast switching dual-frequency liquid crystal optical retarder, driven by an amplitude and frequency modulated voltage," *Appl. Phys. Lett.* 83, 3864–3866 (2003).
- [3] Hsiao, Y.-C., Wu, C.-Y., Chen, C.-H., Zyryanov, V. Ya. and Lee, W., "Electro-optical device based on photonic structure with a dual-frequency cholesteric liquid crystal," *Opt. Lett.* 36, 2632–2634 (2011).
- [4] Pishnyak, O., Sato, S. and Lavrentovich, O. D., "Electrically tunable lens based on a dual-frequency nematic liquid crystal," *Appl. Opt.* 45, 4576–4582 (2006).
- [5] Golovin, Andrii B., Sergij V. Shiyankovskii and Lavrentovich O. D., "Fast switching dual-frequency liquid crystal optical retarder, driven by an amplitude and frequency modulated voltage," *Appl. Phys. Lett.* 83, 3864–3866 (2003).
- [6] Hsiao, Y.-C., Hou, C.-T., Zyryanov, V. Ya. and Lee, W., "Multichannel photonic devices based on tristable polymer-stabilized cholesteric textures," *Opt. Express* 19, 23952–23957 (2011).
- [7] Hsiao, Y.-C., Zou, Y.-H., Timofeev, I. V., Zyryanov, V. Ya. and Lee, W., "Spectral modulation of a bistable liquid crystal photonic structure by the polarization effect," *Opt. Mater. Express* 3, 821–828 (2013).



- [8] Hsiao, Y.-C., Tang, C.-Y. and Lee, W., “Fast-switching bistable cholesteric intensity modulator,” *Opt. Express* 19, 9744–9749 (2011).
- [9] Hsiao, Y.-C. and Lee, W., “Fast-switching bistable light shutters based on dual-frequency cholesteric liquid crystals,” 16th Opto-Electronics and Communications Conference 95–96 (2011).
- [10] Lin, F.-C. and Lee, W., “Color-reflective dual-frequency cholesteric liquid crystal displays and their drive schemes,” *Appl. Phys. Express* 4, 112201 (2011).
- [11] Hsiao, Y.-C. and Lee, W., “Lower operation voltage in dual-frequency cholesteric liquid crystals based on the thermodielectric effect,” *Opt. Express* 21, 23927–23933 (2013).
- [12] Liu, H.-H. and Lee, W., “Time-varying ionic properties of a liquid-crystal cell,” *Appl. Phys. Lett.* 97, 023510 (2010).
- [13] Yin, Y., Shiyanovskii, S. V., Golovin, A. B. and Lavrentovich, O. D., “Dielectric torque and orientation dynamics of liquid crystals with dielectric dispersion,” *Phys. Rev. Lett.* 95, 087801 (2005).
- [14] Tang, C.-Y., Huang, S.-M. and Lee, W., “Dielectric relaxation dynamics in a dual-frequency nematic liquid crystal doped with C.I. Acid Red 2,” *Dyes Pig.* 88, 1–6 (2011).
- [15] Cengel, Y. A., Cimbala, J. M. and Turner, R. H., *Fundamentals of Thermal-Fluid Sciences*, 4th ed. (McGraw-Hill, 2011).
- [16] Bergman, T. L., Lavine, A. S., Incropera, F. P. and DeWitt, D. P., *Fundamentals of Heat and Mass Transfer*, 7th ed. (Wiley, New York, 2011).
- [17] Yablonovitch, E., “Inhibited spontaneous emission in solid-state physics and electronics,” *Phys. Rev. Lett.* 58, 2059–2062 (1987).
- [18] John, S., “Strong localization of photons in certain disordered dielectric superlattices,” *Phys. Rev. Lett.* 58, 2486–2489 (1987).
- [19] Yablonovitch, E., Gmitter, T. J., Meade, R. D., Rappe, A. M., Brommer, K. D. and Joannopoulos, J. D., “Donor and acceptor modes in photonic band structure,” *Phys. Rev. Lett.* 67, 3380–3383 (1991).
- [20] Foresi, J. S., Villeneuve, P. R., Ferrera, J., Thoen, E. R., Steinmeyer, G., Fan, S., Joannopoulos, J. D., Kimerling, L. C., Smith, H. I. and Ippen, E. P., “Photonic crystals: putting a new twist on light,” *Nature* 390, 143–149 (1997).
- [21] Park, B., Kim, M., Kim, S. W. and Kim, I. T., “Circularly polarized unidirectional lasing from a cholesteric liquid crystal layer on a 1-D photonic crystal substrate,” *Opt. Express* 17, 12323–12331 (2009).
- [22] Hsiao, Y.-C., Wang, H.-T. and Lee, W., “Thermodielectric generation of defect modes in a photonic liquid crystal,” *Opt. Express* 22, 3593–3599 (2014).
- [23] Hsiao, Y.-C. and Lee, W., “Electrically induced red, green, and blue scattering in chiral-nematic thin films,” *Opt. Lett.* 40, 1201–1203 (2015).